Structural Eng./Earthquake Eng., JSCE, Vol. 13, No. 1, 55s—66s, 1996 April

STUD ARRANGEMENT TO REDUCE FATIGUE CRACKING IN VERTICAL STIFFENERS

Ichiro OKURA[1], Tetsuya SHIOZAKI[2], Yuhshi FUKUMOTO[3] and Atsushi NANJYO[4]

[1]Member, Associate Professor, Dept. of Civil Eng., Osaka University (2-1 Yamadaoka, Suita, Osaka 565, Japan)
[2]Member, Graduate Student, Dept. of Civil Eng., Osaka University
[3]Member of JSCE, Dr. of Eng. and Ph. D., Professor, Dep. of Civil Eng., Osaka University
[4]Member of JSCE, M. Eng., Hanshin Expr. Public Corp. (4-1-3 Kyutaro-cho, Chuo-ku, Osaka 541, Japan)

The arrangement of stud shear connectors to reduce fatigue cracking at the top of plates to connect a cross beam to a main girder, so-called connection plates, and at the top of the vertical stiffeners in plate girder highway bridges is presented. A model for the transfer of load between a concrete slab and a top flange of a main girder is developed. By the finite element analysis in which this load-transfer-model is introduced, the relations between the stud spacing and the local stresses in connection plates and vertical stiffeners are investigated. Combining these relations and the results of the past research provides the arrangement of studs for composite plate girders as well as that of slab anchors for noncomposite plate girders to reduce the fatigue cracking in connection plates and vertical stiffeners.

Key Words: *fatigue, stud shear connector, concrete slab, girder, stiffener, connection plate*

1. INTRODUCTION

In many plate girder highway bridges in the urban areas of Japan, such fatigue cracks as shown in **Fig.1** are detected at the connections of cross beams to main girders[1]. They are classified as follows:

1) Type 1 crack. This crack is initiated either on the bead or at the toe of the end return of the fillet weld between the connection plate and the top flange of a main girder.
2) Type 2 crack. This crack is created at the periphery of the upper cope of the connection plate, and grows diagonally through the connection plate.
3) Type 3 crack. This crack is produced at the toe of the end return of the fillet weld to connect the connection plate to the main girder web, and grows downward along the toe on the connection-plate side.
4) Type 4 crack. This crack is initiated and propagates along the toe on the web side of the fillet weld between the top flange and the main girder web.

These fatigue cracks are also observed at the connections of sway bracings to main girders[1),2),3)].

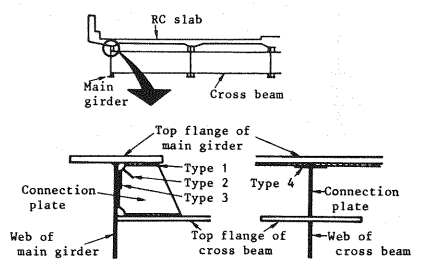

Fig.1 Fatigue cracks at cross-beam connections.

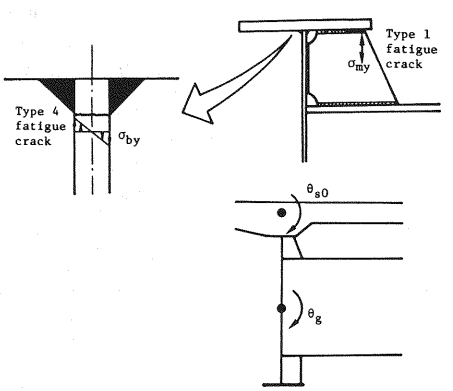

Fig.2 Local stresses and rotations.

This paper is translated into English from the Japanese paper, which originally appeared on J. Struct. Mech. Earthquake Eng., JSCE, No.525/I-33, pp.97-108, 1995.10.

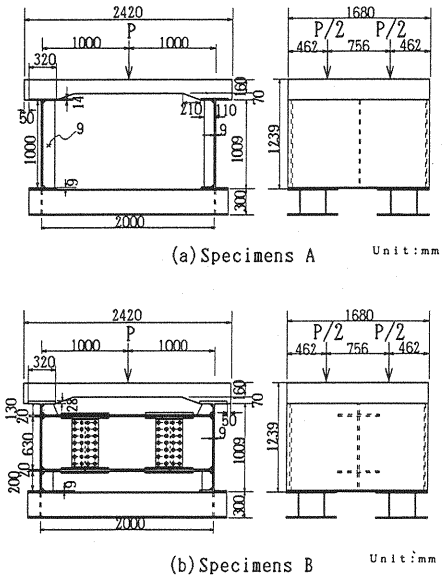

Fig.3 Fatigue test specimens.

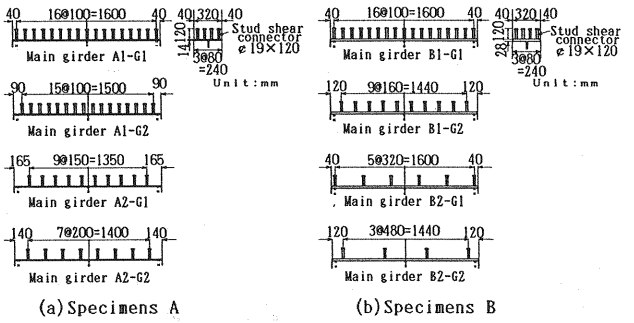

Fig.4 Stud arrangement.

Besides, they are observed at the top of intermediate vertical stiffeners to which neither cross beams nor sway bracings are connected[1]. Therefore, the fatigue cracks in **Fig.1** are typical at the top of the vertical stiffeners of plate girders supporting concrete slabs, whether cross beams and sway bracings exist or not.

From the field stress measurement of an existing plate girder highway bridge, as shown in **Fig.2**, the membrane stress σ_{my} in the vertical direction in the connection plate and the plate-bending stress σ_{by} in the main girder web were found to be governing local stresses to cause Types 1 and 4 fatigue cracks, respectively[4),5)]. These local stresses are produced by the rotation θ_{s0} of a concrete slab due to the slab deformation caused by wheel loads and the rotation θ_g of a cross beam due to the vertical displacements of main girders[6),7)].

The influence of the slab rotation θ_{s0} on the cracking was investigated by the fatigue tests of the specimens consisting of the part above the top flange of a cross beam and a concrete slab 45 cm wide in the bridge-axis direction[8),9),10)]. From the comparison of the results of static loading tests carried out before the fatigue tests and the ones of the finite element analysis of the specimens, it was indicated that eliminating studs (composite plate girders) or slab anchors (noncomposite plate girders) from the locations of the cross-beam connections might decrease the local stresses.

To ensure that, further fatigue tests were done on the specimens consisting of a concrete slab 168 cm wide in the bridge-axis direction, two main girders and a cross beam[11)]. As mentioned before, in actual bridges the fatigue cracks were also observed at the top of intermediate vertical stiffeners. Therefore, specimens without a cross beam were also investigated.

In this paper, analyzing the results of these fatigue tests shows the arrangement of stud shear connectors to reduce the fatigue cracking in connection plates and vertical stiffeners. First, a model for the transfer of load between a concrete slab and a top flange of a main girder is developed. Next, by the finite element analysis in which this load-transfer-model is introduced, the relations between the stud spacing and the local stresses in connection plates and vertical stiffeners are investigated. Finally, combining these relations and the results of the past research provides the arrangement of studs for composite plate girders as well as that of slab anchors for noncomposite plate girders to reduce the fatigue cracking in connection plates and vertical stiffeners.

2. OUTLINE OF FATIGUE TESTS

The specimens of the fatigue tests are shown in **Fig.3**[11)]. A cross beam was used in the specimens B, while it was not used in the specimens A. The interval between the main girders is 2 m. The concrete slab is 168 cm wide in the bridge-axis direction. In the specimens A, vertical stiffeners were provided at three locations at an interval of 80 cm. The slab is 16 cm thick and made from lightweight-aggregate concrete. For each of the specimens A and B, two pieces were prepared. **Fig.4** shows the stud arrangement on the main girders of the specimens. The studs used are 19 mm in diameter and 120 mm in height.

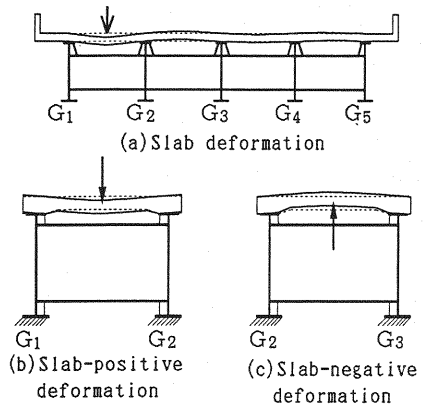

Fig.5 Positive and negative deformations of slab.

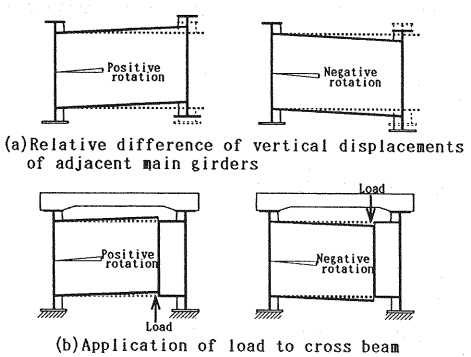

Fig.6 Positive and negative rotations of cross beam.

Static loading tests were conducted ahead of fatigue tests. To examine the relations between the slab deformation and the local stresses, loads of equal magnitude were applied downward at two points 75.6 cm apart in the bridge-axis direction on the top surface of the slab, in the middle between the main girders. Next, the loads were applied upward at the same locations on the bottom surface of the slab. As shown schematically in **Fig.5(a)**, for a load between the main girders G_1 and G_2 in an actual bridge, the slab is deformed in a downward convex form between the main girders G_1 and G_2 and in an upward convex form between the main girders G_2 and G_3. In the static loading tests, the downward and upward convex forms of the slab deformation can be realized by such loading conditions as shown in **Figs.5(b)** and **(c)**, respectively. Here, the slab deformations in **Figs.5(b)** and **(c)** are named slab-positive deformation and slab-negative deformation, respectively.

To investigate the relations between the cross-beam rotation and the local stresses, the bolted connection

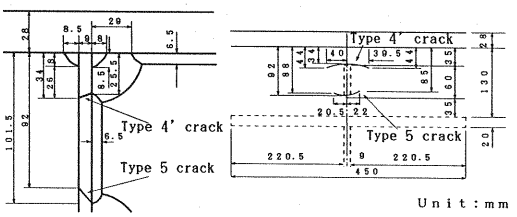

Fig.7 Types 4' and 5 fatigue cracks [Main girder B2-G1].

at one end of the cross beam in the specimens B was undone, and an upward or downward load was applied to this end. As shown in **Fig.6(a)**, positive and negative rotations are produced at the end of a cross beam in an actual bridge, depending on the relative difference of the vertical displacements of adjacent main girders. In the static loading tests, as shown in **Fig.6(b)**, the application of a vertical load to one end of the cross beam causes positive and negative rotations at the other end.

The fatigue tests were accomplished on the specimens A1, B1 and B2 under the slab-positive deformation of **Fig.5(b)**. Type 1 fatigue crack was initiated in the connection plate or the vertical stiffener of each main girder of the three specimens. However, the crack grew very slowly, and stopped after the propagation of about 10 mm. As shown in **Fig.7**, the specimen B1 suffered Type 4' fatigue crack in the web of each main girder, and the specimen B2 experienced Types 4' and 5 fatigue cracks. Types 4' and 5 fatigue cracks were initiated at the toes on the web side of the upper and lower end returns of the fillet weld to connect the connection plate to the main girder web, respectively. Both cracks penetrated the web, and continued to grow horizontally in the web.

3. LOAD-TRANSFER-MODEL BETWEEN SLAB AND TOP FLANGE

In the next chapter, the relations between the stud spacing and the local stresses in connection plates and vertical stiffeners are investigated by a finite element analysis. The model for the transfer of load between a concrete slab and a top flange of a main girder has to be formulated in the way it can be introduced into the finite element analysis.

In the static loading tests, it was observed that as shown in **Fig.8**, the slab rotated at the edges A and B of the top flange of the main girder for the slab-positive and -negative deformations, respectively. Likewise, it was observed that as shown in **Fig.9**, the

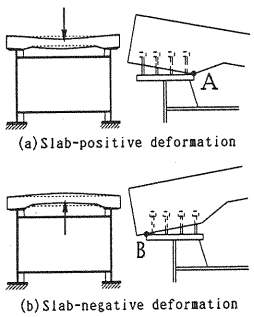

Fig.8 Behavior between slab and flange for slab deformation.

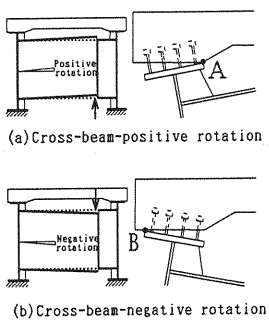

Fig.9 Behavior between slab and flange for cross-beam rotation.

top flange rotated at its edges A and B for the cross-beam-positive and -negative rotations, respectively.

Based on those observations, **Fig.10** shows a load-transfer-model between a concrete slab and a top flange of a main girder. **Fig.10(a)** corresponds to the slab-positive deformation and the cross-beam-positive rotation. **Fig.10(b)** corresponds to the slab-negative deformation and the cross-beam-negative rotation. Plate elements are used in the finite element analysis. In **Fig.10(a)** rigid beams with hinges at both ends connect the nodes on the edge A-A of the neutral plane of the top flange to those on the neutral plane of the slab, and in **Fig.10(b)** they do so on the edge B-B. For the studs, beam elements with the stiffness of the studs join both nodes on the neutral planes of the top flange and the slab.

4. RELATIONS BETWEEN STUD SPACING AND LOCAL STRESSES

(1) Mesh divisions for specimens

Fig.11 shows the mesh divisions for the specimens. **Fig.11(a)** and **(b)** express the mesh divisions for the specimens A and the specimens B with loads applied to the slab, respectively. As was shown in **Fig.4**, the

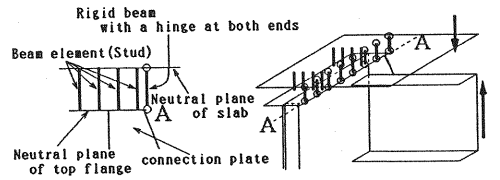

(a) Load-transfer-model for slab-positive deformation and cross-beam-positive rotation

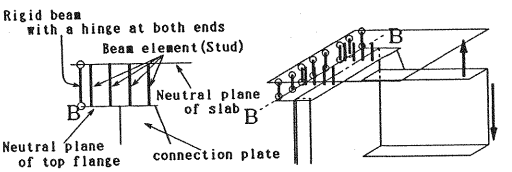

(b) Load-transfer-model for slab-negative deformation and cross-beam-negative rotation

Fig.10 Load-transfer-model between slab and flange.

stud arrangement is different on the right and left main girders of the specimens. Due to the limitations of calculation capacity of the computer, the quarter of the specimen is divided into finite elements. The boundary condition of symmetry was imposed on the cut sections. The bottoms of the web and the vertical stiffener of the main girder were fixed. A uniform load was applied to the slab with the same locations and the same loading areas as adopted in the static loading tests.

Fig.11(c) presents the mesh division for the specimens B with the cross beam loaded. The half of the specimen is divided into finite elements. The two meter long slab was simply-supported at the right-hand edge. A compulsory displacement in the vertical direction was applied to the end of the one meter long cross beam.

The elements used are rectangular and triangular plate elements with 6 degrees of freedom at each node[12]. Rigid beams with hinges at both ends and beam elements with the stiffness of the studs are inserted between the slab and the top flange of the main girder.

(2) Distributions of membrane and plate-bending strains in main girder web

Fig.12 presents the distributions of the membrane strain ε_{my} and plate-bending strain ε_{by} in the vertical direction along the horizontal line 5 cm below the bottom surface of the top flange of the main girder. These are the results of the main girder B1-G1. For the slab-positive deformation, analytical values of

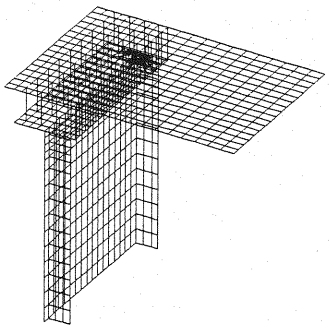

(a) Specimens A

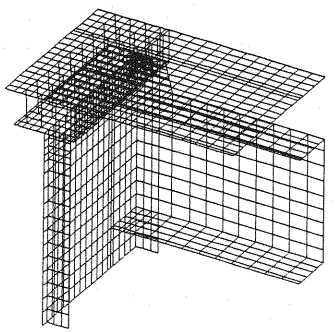

(b) Specimens B with loads applied to slab

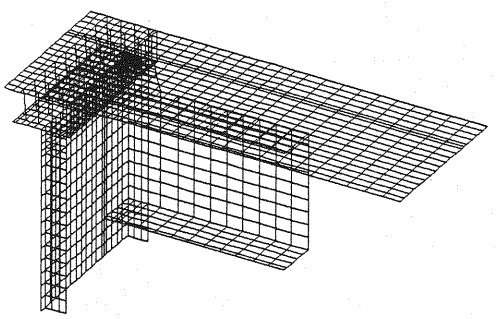

(c) Specimens B with cross beam loaded

Fig.11 Mesh divisions for specimens.

ε_{my} and ε_{by} are close to the respective experimental ones. For the cross-beam-positive rotation, the analytical values of ε_{by} are close to the experimental ones. Although the analytical and experimental values of ε_{my} are a little apart, their tendencies are identical. Therefore, the load-transfer-model developed in the previous chapter deals properly with the transfer of load between a slab and a top flange of a main girder.

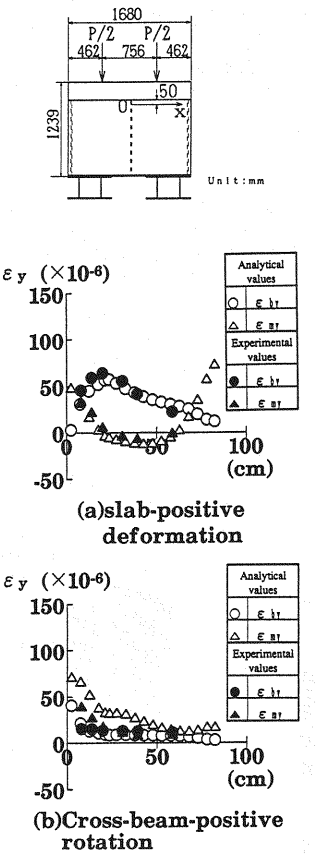

Fig.12 Distributions of ε_{my} and ε_{by} [Main girder B1-G1].

(3) Local strains and stud spacing

Fig.13 demonstrates the local strains in connection plates and vertical stiffeners which will be investigated. In the next section, a comparison is made between the strains obtained from the static loading tests and the finite element analysis. As shown in **Fig.13(a)**, the strains in the static loading tests are as follows:

1) ε_{cy}. This is the strain at the toe on the connection-plate side (or the vertical stiffener side) of the end return of the fillet weld, obtained by linear extrapolation of the strains given by the special strain gauge to measure the stress concentration, so-called stress concentration gauge, glued on the edge of the connection plate (or the vertical stiffener).
2) ε_{sy}. This is the strain at the toe on the web side, provided by linear extrapolation of the strains given by the stress concentration gauge glued on the outside surface of the main girder web.
3) $\varepsilon_{sy'}$. This is the strain at the toe on the web side of

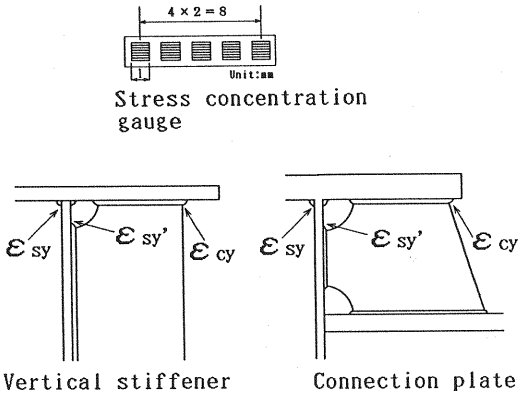

(a) Strains in static loading tests

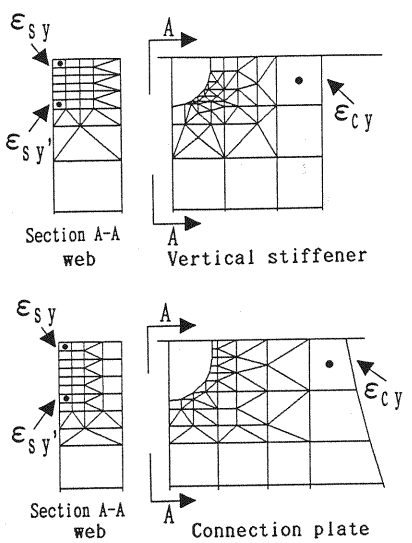

(b) Strains in finite element analysis

Fig.13 Strains in static loading tests and in finite element analysis.

the end return of the fillet weld at the intersection with the cope of the connection plate (or the vertical stiffener), established by linear extrapolation of the strains given by the stress concentration gauge glued on the inside surface of the main girder web.

As shown in **Fig.13(b)**, the strains in the finite element analysis are as follows:

1) ε_{cy}. This is the membrane strain in the vertical direction at the center of the element at the upper right-hand corner of the connection plate (or the vertical stiffener).
2) ε_{sy}. This is the strain in the vertical direction on the outside surface of the main girder web at the center of the element at the upper left-hand corner of the web.
3) $\varepsilon_{sy'}$. This is the strain in the vertical direction on the inside surface of the main girder web at the center of the element of the web at the intersection with the cope of the connection plate (or the vertical stiffener).

The strains ε_{cy} and ε_{sy} are the local strains to cause Types 1 and 4 fatigue cracks, respectively. The strain $\varepsilon_{sy'}$ is the local strain that causes Type 4' fatigue crack.

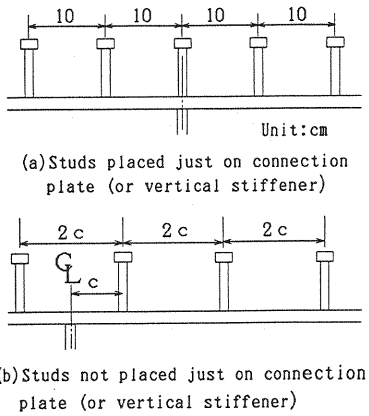

Fig.14 Stud spacing considered in finite element analysis.

Fig.14 shows the stud spacing which was considered in the finite element analysis. In **Fig.14(a)** studs are put just on the connection plate (or the vertical stiffener), and placed at an interval of 10 cm. This arrangement is the same as that of the main girders A1-G1 and B1-G1. In **Fig.14(b)** studs skip over the connection plate (or the vertical stiffener), and are placed at intervals of $2c$=10cm, 20cm, 30cm, 40cm, 50cm, 80 cm, 120cm, 160cm. Accordingly, the distance c from the connection plate (or the vertical stiffener) to its nearest studs is 5cm, 10cm, 15cm, 20cm, 25cm, 40cm, 60cm, 80cm.

(4) Relations between local strains and stud spacing

The relations between the strains $\varepsilon_{cy}, \varepsilon_{sy}, \varepsilon_{sy'}$ and the stud spacing c are presented in **Tables 1, 2** and **3**, respectively. Strain ratios are used for the vertical axis in the figures in the tables. In the analytical values, the denominators $\varepsilon_{0cy}, \varepsilon_{0sy}$ and $\varepsilon_{0sy'}$ are the respective values of $\varepsilon_{cy}, \varepsilon_{sy}$ and $\varepsilon_{sy'}$ for the stud spacing of **Fig.14(a)**. In the experimental values, the strains of the main girders A1-G1 and B1-G1 are

used for ε_{0cy} and ε_{0sy}.

As was shown in **Fig.13**, the locations of the strains in the static loading tests are different from those in the finite element analysis. The finite element analysis does not take the thickness of the top flange and the web of the main girder into consideration. Moreover, it does not take into consideration the fillet welds to connect the connection plate (or the vertical stiffener) to the top flange and the web, and the fillet weld between the top flange and the web. Consequently, as listed in **Table 4**, the magnitudes of the strains given by the static loading tests are greatly different from those by the finite element analysis. Therefore, to enable us to compare the analytical values with the experimental ones, the strain ratios are used for the vertical axis in the figures in **Tables 1, 2** and **3**.

In **Table 4**, the strain values for the slab deformation are at 98 kN which is the sum of the two loads applied to the slab, and the strain values for the cross-beam rotation are at 0.0008 radian of the end rotation of the cross beam. As shown in **Table 4(c)**, the values of $\varepsilon_{0sy'}$ for the slab deformation of the main girder A1-G1 are very small. The values of $\varepsilon_{sy'}$ of the main girders A1-G2 and A2-G1, G2 were also very small. Accordingly, since the experimental values of $\varepsilon_{sy'} / \varepsilon_{0sy'}$ vary largely, they are not plotted in **Table 3**.

As seen in **Tables 1** and **2**, the tendencies of the strain ratios of the analytical and experimental values are identical. Hence, the strains for the stud spacing which was not considered in the static loading tests can be estimated by the finite element analysis.

For the relations between the strain ratios $\varepsilon_{cy} / \varepsilon_{0cy}$, $\varepsilon_{sy} / \varepsilon_{0sy}$, $\varepsilon_{sy'} / \varepsilon_{0sy'}$ and the stud spacing c, the following are pointed out from **Tables 1, 2** and **3**:

For the relation between $\varepsilon_{cy} / \varepsilon_{0cy}$ and c
*(see **Table 1**)*

1) For the slab-positive deformation of the specimens A and B, $\varepsilon_{cy} / \varepsilon_{0cy}$ is almost one, not related to the stud spacing c.
2) For the slab-negative deformation of the specimens A and B, $\varepsilon_{cy} / \varepsilon_{0cy}$ decreases with the increase of the stud spacing c, and it is almost zero for c greater than about 30 cm.
3) For the cross-beam-positive and -negative rotations for the specimens B, $\varepsilon_{cy} / \varepsilon_{0cy}$ decreases gradually, as the stud spacing c increases.

For the relation between $\varepsilon_{sy} / \varepsilon_{0sy}$ and c
*(see **Table 2**)*

1) For the slab-positive deformation of the specimens A and B, $\varepsilon_{sy} / \varepsilon_{0sy}$ decreases, as the stud spacing c increases. Especially, in the specimens A, $\varepsilon_{sy} / \varepsilon_{0sy}$ is almost zero for c greater than about 30 cm.
2) For the slab-negative deformation of the specimens A and B, $\varepsilon_{sy} / \varepsilon_{0sy}$ is above one for c less than about 60 cm. However, $\varepsilon_{sy} / \varepsilon_{0sy}$ sharply decreases for c beyond about 60 cm, and is almost zero at c=80 cm.
3) For the cross-beam-positive rotation of the specimens B, $\varepsilon_{sy} / \varepsilon_{0sy}$ is above one for c less than about 50 cm, and shows the tendency of decrease for c beyond about 50 cm. For the cross-beam-negative rotation, $\varepsilon_{sy} / \varepsilon_{0sy}$ decreases, as the stud spacing c increases, and it becomes almost 0.7 for c above about 30 cm.

For the relation between $\varepsilon_{sy'} / \varepsilon_{0sy'}$ and c
*(see **Table 3**)*

1) The feature in the relation between $\varepsilon_{sy'} / \varepsilon_{0sy'}$ and c is the same as that in the relation between $\varepsilon_{sy} / \varepsilon_{0sy}$ and c.

5. ARRANGEMENT OF STUDS AND SLAB ANCHORS TO REDUCE CRACKING

Combining the results of the past research and the relations between the stud spacing and the local strains obtained in the pervious chapter shows the arrangement of studs (composite plate girders) and slab anchors (noncomposite plate girders) to reduce fatigue cracking in connection plates and vertical stiffeners.

(1) Relation between cracks in vertical stiffeners and stud spacing

As shown in **Table 4(b)**, the experimental values of ε_{0sy} for the slab-positive and -negative deformations of the main girder A1-G1 are 154μ and -172μ, respectively. Both absolute values are close to each other. As shown in **Table 2**, for the slab-positive deformation of the specimens A, $\varepsilon_{sy} / \varepsilon_{0sy}$ decreases with the increase of the stud spacing c. For the slab-negative deformation, however, $\varepsilon_{sy} / \varepsilon_{0sy}$ is above one for c below about 60 cm, and the experimental values of $\varepsilon_{sy} / \varepsilon_{0sy}$ reach to about two. For $\varepsilon_{sy} / \varepsilon_{0sy} = 2$, ε_{sy} is -344μ (= $-172\mu \times 2$). This

Table 1 Relation between $\varepsilon_{cy}/\varepsilon_{0cy}$ and c.

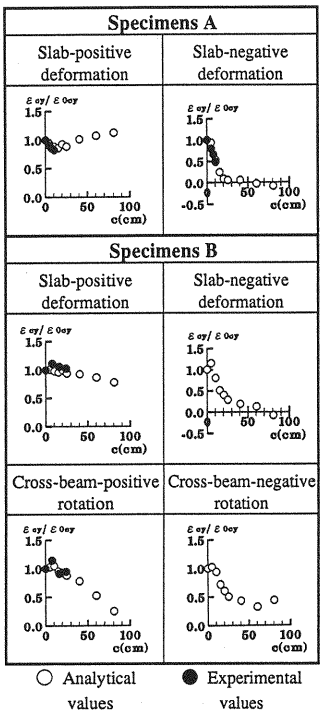

Table 2 Relation between $\varepsilon_{sy}/\varepsilon_{0sy}$ and c.

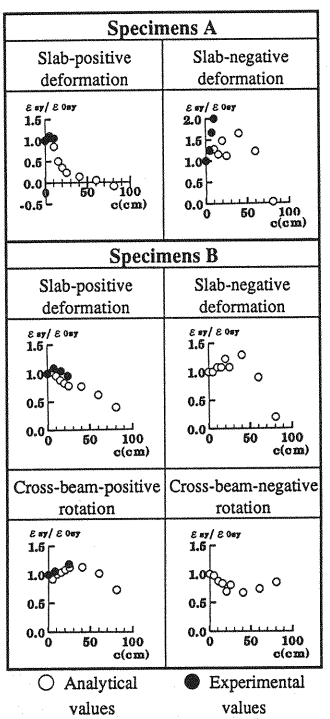

Table 3 Relation between $\varepsilon_{sy'}/\varepsilon_{0sy'}$ and c.

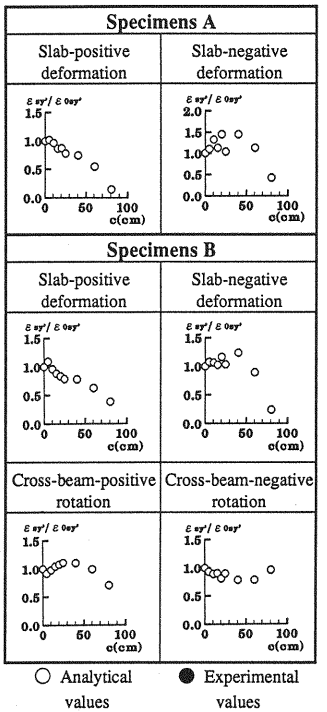

Table 4 Strain values by static loading tests and by finite element analysis.

(a) ε_{0cy} ($\times 10^{-6}$)

Main girder A1-G1		
	Slab-positive deformation	Slab-negative deformation
Experimental values	-1385	1217
Analytical values	-479	436
Main girder B1-G1		
	Slab-positive deformation	Slab-negative deformation
Experimental values	-1146	———
Analytical values	-580	397
	Cross-beam-positive rotation	Cross-beam-negative rotation
Experimental values	-595	———
Analytical values	-515	437

(b) ε_{0sy} ($\times 10^{-6}$)

Main girder A1-G1		
	Slab-positive deformation	Slab-negative deformation
Experimental values	154	-172
Analytical values	316	-353
Main girder B1-G1		
	Slab-positive deformation	Slab-negative deformation
Experimental values	670	———
Analytical values	422	-479
	Cross-beam-positive rotation	Cross-beam-negative rotation
Experimental values	38	———
Analytical values	-230	194

(c) $\varepsilon_{0sy'}$ ($\times 10^{-6}$)

Main girder A1-G1		
	Slab-positive deformation	Slab-negative deformation
Experimental values	16	-6
Analytical values	133	-152
Main girder B1-G1		
	Slab-positive deformation	Slab-negative deformation
Experimental values	———	———
Analytical values	339	-369
	Cross-beam-positive rotation	Cross-beam-negative rotation
Experimental values	———	———
Analytical values	-207	188

absolute value is about half of 670μ, which is the experimental value of ε_{0sy} for the slab-positive deformation of the main girder B1-G1 in **Table 4(b)**. In the main girder B1-G1, Type 4 fatigue crack did not occur due to the local strain ε_{0sy}. Hence, the possibility of initiation of Type 4 fatigue cracks may be low in the specimens A.

As shown in **Table 4(c)**, the values of $\varepsilon_{0sy'}$ for the slab-positive and -negative deformations of the main girder A1-G1 are 16μ and -6μ, respectively. As seen in Table 3, for the slab-positive deformation of the specimens A, $\varepsilon_{sy'} / \varepsilon_{0sy'}$ decreases as the stud spacing c increases. For the slab-negative deformation, however, it is above one for c below about 60 cm, and its maximum value is about 1.5. For $\varepsilon_{sy'} / \varepsilon_{sy} = 1.5$, $\varepsilon_{sy'}$ is -9μ (= $-6\mu \times 1.5$). Type 4' fatigue crack due to the local strain $\varepsilon_{sy'}$ can not be created at this strain level.

From the above it could be inferred that the propagation of Type 1 fatigue crack, the break between the top of vertical stiffeners and the top flange of main girders, increases local stresses in main girder webs, followed by the initiation of Type 4 or 4' fatigue cracks. Accordingly, the stud spacing to decrease the local strain ε_{cy} is required to reduce Type 1 fatigue cracks.

As shown in **Table 4(a)**, for the slab-positive and -negative deformations of the main girder A1-G1, the experimental values of ε_{0cy} are -1385μ and 1217μ, respectively. Both absolute values are close to each other. As seen in **Table 1**, for the slab-positive deformation of the specimens A, $\varepsilon_{cy} / \varepsilon_{0cy}$ is almost one, not related with the stud spacing c. Therefore, for the slab-positive deformation, the stud spacing is of no effect on the local strain ε_{cy}. On the other hand, for the slab-negative deformation of the specimens A, $\varepsilon_{cy} / \varepsilon_{0cy}$ decreases rapidly as the stud spacing c increases, and becomes almost zero for c beyond about 20 cm. Thus, for the slab-negative deformation, enlarging the stud spacing decreases the local strain ε_{cy}, leading to reduction of Type 1 fatigue cracks.

As drawn schematically in **Fig.15(a)**, when a load is between the main girders G_1 and G_2 in a bridge with five main girders, the slab rotations on the main girders G_3, G_4 and G_5 are much smaller than those on the main girders G_1 and G_2[6),7)]. The top of the vertical stiffener of the main girder G_1 is subjected to the slab-positive deformation, and that of the main girder G_2 is under the slab-negative deformation. Likewise, as seen in **Fig.15(b)**, when a load is between the main girders G_2 and G_3, the slab rotations on the main girders G_1, G_4 and G_5 are much smaller than those on the main girders G_2 and G_3[6),7)]. The top of the vertical stiffener of the main girder G_2 is subjected to the slab-positive deformation, and that of the main girder G_3 is under the slab-negative deformation. Thus, in actual bridges, the top of vertical stiffeners of exterior main girders is always subjected to the slab-positive deformation alone, and that of interior main girders is under the slab-positive and -negative deformations.

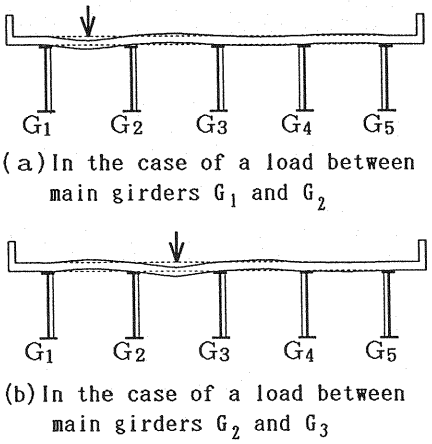

Fig.15 Vertical stiffeners subjected to slab-deformation.

Taking into account the aforementioned relation between the stud spacing and Type 1 fatigue cracks, the enlargement of the stud spacing has no effects on the reduction of Type 1 fatigue cracks in the vertical stiffeners of exterior main girders in actual bridges. For vertical stiffeners of interior main girders, however, the enlargement of the stud spacing reduces Type 1 fatigue cracks, since it decreases the local strain ε_{cy} corresponding to the slab-negative deformation.

(2) Relation between cracks in connection plates and stud spacing

In the past research, it was found that at cross-beam connections to exterior main girders, Types 1 and 4 fatigue cracks are initiated independently, and that at cross-beam connections to interior main girders, the propagation of Type 1 fatigue cracks induces local stresses in main girder webs, followed by Type 4 fatigue cracks[8),9),10)]. Besides, it was discovered that for Type 1 fatigue cracks, the slab rotation alone is dominant, and that for Type 4 fatigue cracks, the slab and cross-beam rotations are both influential[13),14),15)].

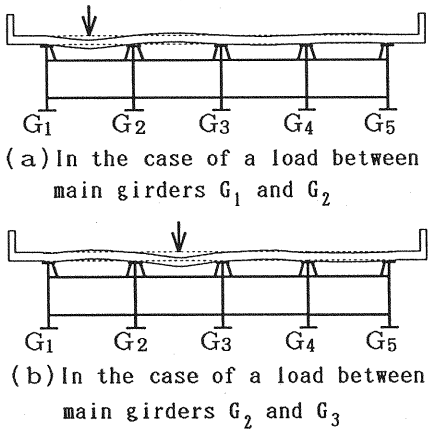

Fig.16 Connection plates subjected to slab-deformation.

From these facts, for connection plates of exterior main girders, the stud spacing to decrease the respective strains ε_{cy}, ε_{sy}, $\varepsilon_{sy'}$ for Types 1, 4 and 4' fatigue cracks is investigated. For connection plates of interior main girders, the stud spacing to decrease the strain ε_{cy} is studied. For the local strain ε_{cy}, only the slab deformation is influential. For the local strains ε_{sy} and $\varepsilon_{sy'}$, the slab deformation and cross-beam rotation are both effective.

As seen in **Fig.16(a)**, when a load is between the main girders G_1 and G_2 in a bridge with five main girders, the slab rotations on the main girders G_3, G_4 and G_5 are much smaller than those on the main girders G_1 and G_2[6),7)]. The connection plate of the main girder G_1 and the connection plate on the left-hand side of the main girder G_2 are subjected to the slab-positive deformation, and the connection plate on the right-hand side of the main girder G_2 is under the slab-negative deformation. As seen in **Fig.16(b)**, when a load is between the main girders G_2 and G_3, the slab rotations on the main girders G_1, G_4 and G_5 are much smaller than those of the main girders G_2 and G_3[6),7)]. The connection plate on the right-hand side of the main girder G_2 and the connection plate on the left-hand side of the main girder G_3 are subjected to the slab-positive deformation, and the connection plate on the left-hand side of the main girder G_2 and the connection plate on the right-hand side of the main girder G_3 are under the slab-negative deformation.

Cross beams rotate in the positive or negative direction at exterior main girders, depending on the relative difference of vertical displacements of the exterior main girders and their adjacent interior main girders.

Therefore, the local strain ε_{cy} in connection plates of exterior main girders is produced by the slab-positive deformation alone, and ε_{cy} in connection plates on the right and left sides of interior main girders is created by the slab-positive and -negative deformations. The local strains ε_{sy} and $\varepsilon_{sy'}$ in webs of exterior main girders are induced by the slab-positive deformation and the cross-beam-positive and -negative rotations.

As shown in **Table 1**, for the slab-positive deformation of the specimens B, $\varepsilon_{cy} / \varepsilon_{0cy}$ is almost one, not related with the stud spacing c. This means that for exterior main girders, enlarging the stud spacing is of no effect on the reduction of Type 1 fatigue cracks in connection plates. For the slab-negative deformation of the specimens B, $\varepsilon_{cy} / \varepsilon_{0cy}$ decreases rapidly with the increase of the stud spacing c, and takes 0.3 at c=25cm. Hence, for interior main girders, the enlargement of the stud spacing reduces Type 1 fatigue cracks, since it decreases the local strain ε_{cy} corresponding to the slab-negative deformation.

As shown in **Tables 2** and **3**, for the slab-positive deformation of the specimens B, $\varepsilon_{sy} / \varepsilon_{0sy}$ and $\varepsilon_{sy'} / \varepsilon_{0sy'}$ decrease gradually, as the stud spacing c increases. For the cross-beam-positive rotation, however, $\varepsilon_{sy} / \varepsilon_{0sy}$ and $\varepsilon_{sy'} / \varepsilon_{0sy'}$ are above one for c below about 50 cm. Thus, for exterior main girders, the effects of the enlargement of the stud spacing on the reduction of Types 4 and 4' fatigue cracks depend on the magnitudes of the slab-positive deformation and the cross-beam-positive rotation caused in actual bridges.

(3) Arrangement of studs (composite plate girders) and slab anchors (noncomposite plate girders) to reduce fatigue cracking in connection plates and vertical stiffeners

As was mentioned in the previous sections, for interior main girders, Type 1 fatigue cracks can be reduced by keeping studs away from the locations of vertical stiffeners and connection plates.

The stud spacing is according to the design of shear connectors of composite girders. It is determined so as to resist the shear force in the bridge-axis direction between a top flange of a steel girder and a concrete slab. Hence, in order to reduce Type 1 fatigue cracks in interior main girders of composite plate girder bridges, studs should be placed as far as possible from the locations of vertical stiffeners and connection plates. The stud spacing is determined by the design of shear connectors of composite girders.

In the past fatigue tests, such fatigue cracks as shown in Fig.1 also occurred in the specimens where slab anchors were used[8),9),10)]. The fatigue cracks can be initiated in noncomposite plate girder bridges. In order to reduce Type 1 fatigue cracks in interior main girders in noncomposite plate girder bridges, slab anchors should be placed as far as possible from the locations of vertical stiffeners and connection plates.

Placing studs (composite plate girders) and slab anchors (noncomposite plate girders) away from the locations of vertical stiffeners and connection plates do not require any additional costs in fabrication of plate girders.

6. CONCLUSIONS

The arrangement of studs (composite plate girders) and slab anchors (noncomposite plate girders) to reduce fatigue cracking in connection plates and vertical stiffeners in plate girder highway bridges was investigated. The main results are as follows:

(1) At the top of intermediate vertical stiffeners where neither cross beams nor sway bracings are connected, the propagation of Type 1 fatigue cracks causes the break between the top of vertical stiffeners and the top flange of main girders, which increases local stresses in main girder webs, and is followed by Type 4 or 4' fatigue cracks. Therefore, the prevention of Type 1 fatigue cracks leads to that of other fatigue cracks. For interior main girders, enlarging the stud spacing is effective for reducing Type 1 fatigue cracks. For exterior main girders, however, it is not.

(2) At cross-beam connections to exterior main girders, Type 1 fatigue cracks in connection plates and Types 4 and 4' fatigue cracks in main girder webs occur independently. For exterior main girders, the enlargement of the stud spacing is of no effect on the reduction of Type 1 fatigue cracks, and the effects of enlarging the stud spacing on the reduction of Types 4 and 4' fatigue cracks depend on the magnitudes of the slab-positive deformation and the cross-beam-positive rotation caused in actual bridges. At cross-beam connections to interior main girders, the propagation of Type 1 fatigue cracks increases local stresses in main girder webs, and induces Type 4 fatigue cracks. Hence, at cross-beam connections to interior main girders, the prevention of Type 1 fatigue cracks results in that of other fatigue cracks. For interior main girders, the enlargement of the stud spacing reduces Type 1 fatigue cracks.

(3) Summarizing the above, enlarging the stud spacing has an effect on the reduction of the fatigue cracks in connection plates and vertical stiffeners of interior main girders, but it does not for exterior main girders.

(4) Based on these results, the arrangement of studs (composite plate girders) and slab anchors (noncomposite plate girders) to reduce the fatigue cracking in connection plates and vertical stiffeners of interior main girders is as follows: For composite plate girders, studs should be placed as far as possible from the locations of vertical stiffeners and connection plates. The stud spacing is determined by the design of shear connectors of composite girders. For noncomposite plate girders, slab anchors should be placed as far as possible from the locations of vertical stiffeners and connection plates.

REFERENCES

1) Okura, I.: *Fatigue in Steel Bridges,* Toyo-shoten Publisher, Tokyo, Japan, 1994. (in Japanese)
2) Kato, S., Yoshikawa, O., Terada, H. and Matsumoto, Y.: Studies on fatigue damages based on strain measurement of a highway bridge, *J. Structural Engrg./Earthquake Engrg.*, JSCE, Japan, Vol.2, No.2, pp.445-454, 1985.
3) Miki, C., Takenouchi, H., Mori, T. and Ohkawa, S.: Repair of fatigue damage in cross bracing connections in steel girder bridges, *J. Structural Engrg./Earthquake Engrg.*, JSCE, Japan, Vol.6, No.1, pp.31-39, 1989.
4) Okura, I., Hirano, H. and Yubisui, M.: Stress measurement at cross beam connections of plate girder bridge, *Tech. Reports of Osaka Univ.*, Osaka Univ., Osaka, Japan, Vol.37, No.1883, pp.151-160, 1987.
5) Okura, I. and Fukumoto, Y.: Fatigue of cross beam connections in steel bridges, *Proc., IABSE 13th Congress*, Helsinki, Finland, pp.741-746, 1988.
6) Okura, I., Yubisui, M. and Hirano, H.: Relation between local stresses at cross beam connection and three dimensional behavior of plate girder bridge, *J. Structural Engrg.*, Vol.33A, pp.373-382, 1987. (in Japanese)
7) Okura, I., Yubisui, M., Hirano, H. and Fukumoto, Y.: Local stresses at cross beam connections of plate girder bridges, *J. Structural Engrg./Earthquake Engrg.*, JSCE, Japan, Vol.5 No.1, pp.89-97, 1988.
8) Okura, I. and Fukumoto, Y.: Fatigue of cross-beam connections in plate girder highway bridges, *Proc., IABSE Workshop*, Lausanne, Switzerland, pp.167-176, 1990.
9) Okura, I. Inoue, H., Fukumoto, Y. and Yamada, Y.: Fatigue tests of cross-beam connections in plate girder highway bridges, *J. Structural Engrg.*, Japan, Vol.38A, pp.989-998, 1992. (in Japanese)
10) Okura, I. and Fukumoto, Y.: Fatigue tests of cross-beam connections in plate girder highway bridges, *Proc., First World Conference on Constructional Steel Design*, Acapulco, Mexico, pp.466-469, 1992.
11) Okura, I., Sakamoto, H., Shiozaki, T., Fukumoto, Y. and Nanjyo, A.: Local stresses and fatigue cracks at the top of vertical stiffeners of plate girders, *J. Structural Engrg.*,

Japan, Vol.40A, pp.1087-1100, 1994. (in Japanese)
12) ISAP(Integrated Structural Analysis Program), NEC Corporation, FXI 52-10, Tokyo, Japan, 1989.
13) Okura, I., Takigawa, H. and Fukumoto, Y.: Structural parameters governing fatigue cracking at cross-beam connections in plate girder highway bridges, *Tech. Reports of Osaka Univ.*, Osaka Univ., Osaka, Japan, Vol.39, No.1980, pp.289-296, 1989.
14) Okura, I., Takigawa, H. and Fukumoto, Y.: Structural parameters governing fatigue in highway bridges, *J. Structural Engrg./Earthquake Engrg.*, JSCE, Japan, Vol.6, No.2, pp.423-426, 1989.
15) Okura, I., Takigawa, H. and Fukumoto, Y.: Structural parameters governing fatigue cracks at cross-beam connections of plate girder bridges, *J. Structural Engrg.*, Japan, Vol.35A, pp.921-928, 1989. (in Japanese)